applied optics

Analytical investigation of the parasitic diffraction orders of tilt carrier frequency computer-generated holograms

Jiantao Peng,[1,2,*] Jianyue Ren,[1] Xingxiang Zhang,[1] and Zhe Chen[1,2]

[1]Changchun Institute of Optics, Fine Mechanics and Physics, Chinese Academy of Science, Changchun 130033, China
[2]University of Chinese Academy of Sciences, Beijing 100049, China
*Corresponding author: jtpeng1989@163.com

Received 26 January 2015; revised 30 March 2015; accepted 31 March 2015; posted 1 April 2015 (Doc. ID 233195); published 24 April 2015

Computer-generated holograms (CGHs) are commonly used to test aspheric surfaces. In order to eliminate the influence of spurious diffraction orders, adequate carrier frequency is applied to CGHs to separate the overlapping orders. This paper describes a paraxial parametric model for separating the parasitic diffraction orders of a tilt carrier frequency CGH placed outside the interferometer focus. The approximate analytical expression for the disturbing field on the filter plane is derived using the paraxial model. This expression provides a recipe for determining the amount of tilt carrier frequency needed to eliminate the disturbing orders, and is applicable to concave weak aspheric surfaces with large f-numbers of the best-fit spheres, where paraxial approximation is valid. CGH design examples are provided.

OCIS codes: (090.1760) Computer holography; (120.4630) Optical inspection; (220.1250) Aspherics.

http://dx.doi.org/10.1364/AO.54.004033

1. INTRODUCTION

Computer-generated holograms (CGHs) used for aspheric surface testing have evolved into standard practice in high-precision metrology [1–4]. The spurious diffraction orders of the CGH along with the desired order result in overall interferograms of low quality, and sometimes make the measurement impossible [5].

Power or tilt carrier frequency is employed to separate the diffraction orders [6–8]. Enough carrier frequency must be applied to the CGH to spatially isolate the wanted order, followed by a pinhole placed at the focal plane to block the unwanted ones. However, superfluous carrier frequency merely decreases the line spacing of the CGH, thus driving the cost up and the accuracy down [9,10]. Searching for an admissible carrier frequency within the fabrication limits is one of the designers' destinies.

The characterization of separating the parasitic diffraction orders varies with the CGH position (Fig. 1) [11]. The CGH placed outside the interferometer focus averts the restriction of the interferometer aperture and the unknown working state of the inner filter of a commercial interferometer. However, in this case, all the diffraction orders during the first passage of the CGH pass through the CGH again and are divided into different diffraction-order combinations [Fig. 1(b)], while when the CGH is placed inside the focus, only the desired order (+1 order) during the first passage passes the CGH a second time [Fig. 1(a)]. Hence, the CGH placed outside the interferometer focus has a more complicated diffraction property than the CGH placed inside the focus and needs auxiliary analysis with optical software. The amount of carrier frequency is usually gained with the method of trial and error.

CGHs with tilt carriers surmount the well-known obstacles that CGHs with power carriers suffer from the disturbing interferences on axis, hence the central parts of the test surfaces are measured inaccurately. Thus, tilt carrier frequency is often applied to CGHs when aspherics with no central obscuration are under test. The diffraction orders must be fanned out, enabling the isolation of a pure test or reference beam. Lindlein [12] analyzed the disturbing effects of the CGH placed outside the focus and achieved an approximate expression for the spatial frequencies of the unwanted diffraction orders. But the expression was only adaptive to the case when the CGH is close to the aspheric surface. Garbusi and Osten [13] obtained an analytical expression for the stray field on the detector. But the double-pass undesired orders were not considered. Zhou *et al.* [14] proposed a paraxial solution for the amount of the needed power carrier frequency, but the CGH with tilt carriers was not discussed.

When a concave aspheric surface is under test, the CGH is usually placed near the focal point of the interferometer to achieve a small size and hence a low cost, under the trade-off among the cost, the line spacing and the mapping error. For

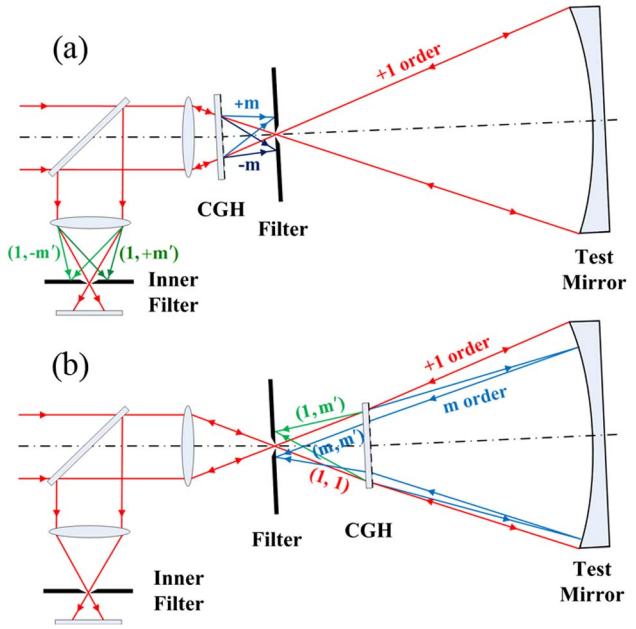

Fig. 1. Schematic of test configurations. (a) The CGH is placed inside the interferometer focus. Disturbing diffraction orders are blocked by the filter and the inner filter of the commercial interferometer. (b) The CGH is placed outside the focus. All the diffraction orders are reflected by the test mirror and diffracted again by the CGH. The filter alone selects the desired measurement order.

optical testing of a concave weak aspheric surface (e.g., $-0.5 \le K \le 0$, where K is the conic constant) with a large $F/\#$ ($F/\# \ge 2$), the purpose of this paper is to establish a recipe for determining the amount of tilt carrier frequency needed to eliminate the unwanted waves for the CGH placed outside the interferometer focus. We consider the influence of the CGH position and the double-pass undesired orders, and derive an analytical expression for the disturbing field on the filter plane using a parametric geometric model under the paraxial optics approximation. In Section 2, the phase function of the tilt carrier frequency CGH used for testing a concave weak conic surface with a large $F/\#$ is achieved, and a paraxial solution for the amount of the needed tilt carrier frequency is obtained. In Section 3, the necessary condition for separating the spurious diffraction orders is discussed, and the theory is extended to concave weak aspherics and off-axis aspherics with large $F/\#$. In Section 4, a detailed comparison between the paraxial solution and the Zemax-based ray trace is done, and finally, CGH design examples are exhibited.

2. PARAMETRIC MODEL AND THEORETICAL DERIVATION

A. Phase Function of the Tilt Carrier Frequency CGH

For optical testing of concave conic surfaces, assuming that the conic constant K is small and the $F/\#$, defined as $R/2D$, is large such that paraxial optics are satisfied, a parametric geometric model is constructed by ignoring the thickness of the CGH glass plate to derive the phase function of the CGH with tilt carriers (Fig. 2). The CGH is placed outside the interferometer focus, distance h away from the paraxial focus C of the test

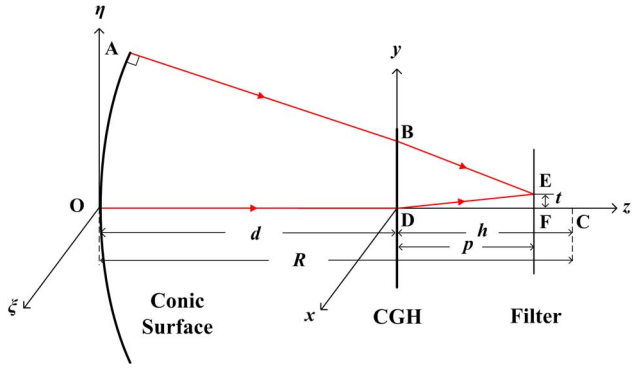

Fig. 2. Schematic of the parametric geometric model. A conic surface with a radius of curvature R and an aperture D is under test using a CGH with tilt carriers. The point C is the paraxial focus of the test surface. The parameters d, h, p, and t are defined as shown. The value of t/p denotes the amount of tilt carrier frequency.

conic surface to avoid the caustic area. Rays that are perpendicular to the test mirror are traced, since CGHs are employed to convert standard spherical wavefronts from interferometers to aspheric wavefronts that match the test mirrors. The CGH phase function is gained by computing the optical path difference between the propagating rays.

The phase function of the CGH without tilt carriers in the cylindrical coordinate is achieved by Zhou *et al.* [15] as

$$\begin{aligned}\Phi(r_m) &= OD + DF - AB - BF \\ &= \frac{(-h^2 + hp)}{2pR^2} r_m^2 + \frac{r_m^4}{8p^3R^4}(h^4 - 4h^2p^2 - 4h^2Kp^2 \\ &\quad + 3hp^3 + 4hKp^3 + 4hKp^2R - 3Kp^3R), \end{aligned} \tag{1}$$

where R is the radius of curvature, K is the conic constant, $r_m = (\xi^2 + \eta^2)^{1/2}$ is the radial position on the conic surface, and p is the distance from the CGH to the filter.

We derive Eq. (1) up to the sixth order and represent it with respect to the CGH coordinate (x, y) for convenience in the following discussion. When $h, p \ll R$, which is true in most cases, and when the approximation $r_m^6/R^6 \approx r^6/h^6$ is adopted, the phase function of the CGH without tilt carriers is further simplified as

$$\Phi(r) = \frac{1}{2}\left(\frac{1}{h} - \frac{1}{p}\right) r^2 + \frac{KR}{8h^4} r^4 + \frac{K^2R^2}{8h^7} r^6, \tag{2}$$

where $r = (x^2 + y^2)^{1/2}$ is the radial position on the CGH.

When the tilt carrier frequency is loaded to the CGH, the focus of the rays is shifted from the point F to E. Assuming that the ratio t/p is small such that any term with t^2/p^2 is inconsequential, the CGH phase function is written as

$$\begin{aligned}\Phi(x, y) &= OD + DE - AB - BE \\ &= \frac{t}{p} y + \frac{1}{2}\left(\frac{1}{h} - \frac{1}{p}\right)(x^2 + y^2) - \frac{t}{2p^3}(x^2 + y^2)y \\ &\quad + \frac{KR}{8h^4}(x^2 + y^2)^2 + \frac{3t}{8p^5}(x^2 + y^2)^2 y \\ &\quad + \frac{K^2R^2}{8h^7}(x^2 + y^2)^3. \end{aligned} \tag{3}$$

In Eq. (3) the first four terms have the form of tilt, defocus, coma, and the third-order spherical aberration, respectively. It reveals that the CGH has a certain power unless $p = h$, and coma aberration is brought in along with tilt carriers.

B. Separated Distances of the Undesired Diffraction Orders

The propagation of the diffraction orders of the CGH placed outside the interferometer focus is shown in Fig. 3. Paraxial optics are considered. The included angle β between the propagating direction of the undesired wavefront and that of the desired wavefront is described by Lindlein [12] as

$$\beta_x = (m+m'-2)\frac{\partial\Phi}{\partial x} + 2(m'-1)\left(\Delta x\frac{\partial^2\Phi}{\partial x^2} + \Delta y\frac{\partial^2\Phi}{\partial x\partial y}\right),$$
$$\beta_y = (m+m'-2)\frac{\partial\Phi}{\partial y} + 2(m'-1)\left(\Delta y\frac{\partial^2\Phi}{\partial y^2} + \Delta x\frac{\partial^2\Phi}{\partial x\partial y}\right), \quad (4)$$

with

$$\Delta x = (m-1)d(x,y)\frac{\partial\Phi}{\partial x},$$
$$\Delta y = (m-1)d(x,y)\frac{\partial\Phi}{\partial y}, \quad (5)$$

where $\Phi = \Phi(x,y)$ is the phase function of the CGH, $d(x,y)$ is the length of the ray from the CGH to the test mirror, and the subscripts x and y denote the corresponding components. Only the diffraction-order combination $(m,m') = (1,1)$ is the desired order for testing.

In fact, Eq. (5), given by Lindlein, is an approximation which is valid only when the CGH is placed close to the test mirror. When the distance between the CGH and the test mirror is not ignorable, we propose an approximate expression that includes the influence of the CGH position:

$$\Delta x = (m-1)\frac{hd}{R}\frac{\partial\Phi}{\partial x},$$
$$\Delta y = (m-1)\frac{hd}{R}\frac{\partial\Phi}{\partial y}. \quad (6)$$

The derivation of Eq. (6) is shown in Appendix A.

The separated distance Δl between the diffraction order (1, 1) and (m,m') on the filter plane is depicted by EE′, which is calculated under paraxial optics consideration and presented as

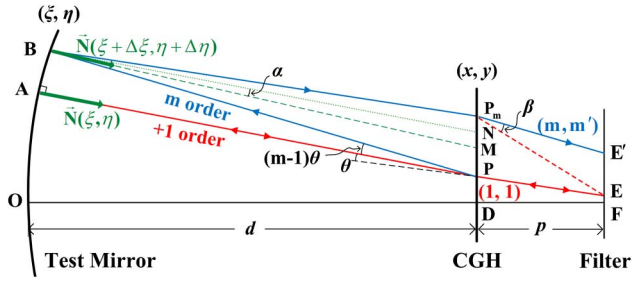

Fig. 3. Propagation of the diffraction orders. A ray is divided into the orders +1 and m at the point P(x,y), reflected by the aspheric mirror at the point A(ξ,η) and B$(\xi+\Delta\xi,\eta+\Delta\eta)$ separately, then diffracted again by the CGH at the point P(x,y) and P$_m(x+2\Delta x, y+2\Delta y)$. **N** is the local surface normal vector. BN is parallel to AP. θ, α, and β are the included angles as shown.

$$\Delta l_x = p\beta_x,$$
$$\Delta l_y = p\beta_y. \quad (7)$$

The component Δl_y is emphasized since the tilt carrier frequency is applied along the y direction. Rays on the meridional plane are analyzed first, where the coordinate (x,y) and (ξ,η) are simplified to $(0,y)$ and $(0,\eta)$. Thus, $\Delta l_x = 0$, and Δl_y is described as

$$\Delta l_y = (m+m'-2)p\frac{\partial\Phi}{\partial y} + 2(m-1)(m'-1)\frac{phd}{R}\frac{\partial\Phi}{\partial y}\frac{\partial^2\Phi}{\partial y^2}. \quad (8)$$

Equation (8) indicates that the rays with order $m+m'=2$ are stubbornly hard to eliminate since in this case the first term vanishes, which has been shown in Lindlein's work.

The stubborn rays with order $m+m'=2$ are studied first. By normalizing the variable y with the semi-aperture of the CGH, i.e., r_{CGH}, and with the help of the phase function of Eq. (3), the detached distance Δl_y of the stubborn rays is expanded and simplified as

$$\Delta l_y(y) = 2(m-1)(m'-1)\frac{(p-h)d}{pR}\{t + a_1 r_{\mathrm{CGH}} y + a_2 r_{\mathrm{CGH}}^2 y^2 t + a_3 r_{\mathrm{CGH}}^3 y^3 + a_4 r_{\mathrm{CGH}}^4 y^4 t\}, \quad (9)$$

with

$$a_1 = \frac{p-h}{h}, \qquad a_2 = \frac{3KRp}{2(p-h)h^3},$$
$$a_3 = \frac{2KRp}{h^4}, \qquad a_4 = \frac{15K^2R^2p}{4(p-h)h^6},$$
$$r_{\mathrm{CGH}} = \frac{hD}{2R} - \frac{KD^3}{16R^2} - \frac{3K(K+1)D^5}{256R^4}, \quad (10)$$

where D is the aperture of the test conic surface. Here $p \neq h$ is forwardly presumed, otherwise $\Delta l_y(0) = 0$, causing the disturbing interferences on axis. In addition, the terms with t^2/p^2 are neglected owing to the supposition that $t \ll p$. The terms with order higher than y^4 are ignored too on the basis of the paraxial optics assumption and the fact that $\partial^2\Phi/\partial y^2$ is approximated to the fourth order.

C. Amount of the Needed Tilt Carrier Frequency

In terms of geometrical optics, a stray ray is able to be eliminated by an ideal pinhole, as long as the distance Δl along the x or y direction on the filter plane is nonzero. Owing to the continuity of the function $\Delta l_y(y)$ and the presumption that $t > 0$, the disturbing diffraction orders are separable only when the value of the grouping of quantities in the brace of Eq. (9) is constantly greater than zero. Thus, the following inequalities are obtained:

$$t + a_1 r_{\mathrm{CGH}} + a_2 r_{\mathrm{CGH}}^2 t + a_3 r_{\mathrm{CGH}}^3 + a_4 r_{\mathrm{CGH}}^4 t > 0,$$
$$t - a_1 r_{\mathrm{CGH}} + a_2 r_{\mathrm{CGH}}^2 t - a_3 r_{\mathrm{CGH}}^3 + a_4 r_{\mathrm{CGH}}^4 t > 0. \quad (11)$$

By solving inequalities (11), the necessary condition for separating the diffraction orders is gained:

$$1 + a_2 r_{\mathrm{CGH}}^2 + a_4 r_{\mathrm{CGH}}^4 > 0. \quad (12)$$

The amount of the needed tilt carrier frequency is described as

$$\frac{t}{p} > \frac{r_{\mathrm{CGH}}}{p}\frac{|a_1 + a_3 r_{\mathrm{CGH}}^2|}{1 + a_2 r_{\mathrm{CGH}}^2 + a_4 r_{\mathrm{CGH}}^4}. \tag{13}$$

In fact, Δl must be larger than a nonzero constant L_0 on account of the diffraction properties of light and the practical precision of fabrication and alignment of the pinhole. Hence, the minimum t is

$$t \geq \frac{|a_1 + a_3 r_{\mathrm{CGH}}^2| r_{\mathrm{CGH}}}{1 + a_2 r_{\mathrm{CGH}}^2 + a_4 r_{\mathrm{CGH}}^4} + \frac{pRL_0}{2|p-h|d(1 + a_2 r_{\mathrm{CGH}}^2 + a_4 r_{\mathrm{CGH}}^4)}. \tag{14}$$

Equation (14) uses the fact that the minimum value of $|(m-1)(m'-1)|$ with the condition $m + m' = 2$ is achieved and equal to 1 when $(m, m') = (0, 2)$ or $(2, 0)$.

3. DISCUSSION

A. In-Depth Discussion on the Necessary Condition

The necessary condition of Eq. (12) is worth further discussion, since if it is not satisfied, the disturbing rays with the order $m + m' = 2$ would be nonremovable no matter how large tilt carrier frequency is adopted.

By approximating r_{CGH} as $hD/2R$ for simplicity, the inequality Eq. (12) is written as the following:

$$1 + \frac{3R}{32(F^{\#})^2 h}\frac{Kp}{p-h}\left(1 + \frac{5KR}{32(F^{\#})^2 h}\right) > 0. \tag{15}$$

Paraxial optics are examined. The parameter h is circumscribed by three elements: the permissible maximum aperture of the CGH, the upper limit of imaging distortion, and the forbidden field of the caustic area. Hence, $|5KR/32(F^{\#})^2 h| < 1$ is the usual case. If $K < 0$ and $p < h$, the inequality Eq. (15) is held automatically.

If $K < 0$ and $p > h$, the value of the left grouping of quantities of inequality Eq. (15) decreases by neutralization, contrary to the target to abate the amount of the needed tilt carrier frequency according to Eqs. (13) and (14), e.g., $K = -0.5$, $F/\# = 2$, $R = 8000$ mm, and $h = 500$ mm, if $p > h$, $p > 574.0$ mm is demanded by inequality Eq. (15). If $p = 600$ mm, $t/p \geq 0.1$ is hence required, resulting in a huge tilt carrier frequency. If $p = 650$ mm, tilt carrier frequency is acceptable, while power carrier frequency, shown as the defocus term in Eq. (3), is conspicuous, in which case the additional tilt carrier frequency is not indispensable.

In summary, when $K < 0$, settling the filter before the paraxial focus, i.e., $p < h$, is a more reasonable choice for the CGH with tilt carriers than setting $p > h$.

B. Extended to a Concave Weak Aspheric Surface with a Large $F/\#$

When a surface with aspheric coefficients is under test, the paraxial solution for the needed t is derived similarly. It has the same form with Eq. (14), except that

$$a_1 = \frac{p-h}{h}, \qquad a_2 = \frac{3(K+a)Rp}{2(p-h)h^3},$$
$$a_3 = \frac{2(K+a)Rp}{h^4}, \qquad a_4 = \frac{15(K^2+a^2)R^2 p}{4(p-h)h^6},$$
$$r_{\mathrm{CGH}} = \frac{hD}{2R} - \frac{(K+a)D^3}{16R^2} - \frac{3[(K+1)K - a + b]D^5}{256R^4}, \tag{16}$$

with

$$a = 8AR^3, \qquad b = 16BR^5, \tag{17}$$

where A is the fourth-order coefficient, and B is the sixth-order coefficient.

Admittedly, for an aspheric surface, the fourth-order coefficient A is coupled with the conic constant K. Thus, the concurrence of A and K is forbidden, and the parameter $a = 8AR^3$ can be treated equivalently as the conic constant K.

C. Extended to a Concave Off-Axis Aspheric Surface with a Weak Aspherical Deformation and a Large $F/\#$

The approximate expression of Eq. (9) is applicable to concave off-axis aspheric surfaces with a weak aspherical deformation and a large $F/\#$, which is defined as the f-number of the mother mirror, as long as the value ranges of y are reset on the basis of the lateral displacements.

Granted a concave off-axis aspheric surface with a lateral displacement equal to its semi-aperture is under test, by redefining r_{CGH} as the maximum value of y in the CGH plane, the value range of y changes to $0 \leq y \leq 1$. The symmetry of the parameter t is broken, thus t is no longer limited to a positive number. The condition for separating the diffraction orders is changed to

$$t \cdot (t + a_1 r_{\mathrm{CGH}} y + a_2 r_{\mathrm{CGH}}^2 y^2 t + a_3 r_{\mathrm{CGH}}^3 y^3 + a_4 r_{\mathrm{CGH}}^4 y^4 t) > 0, \tag{18}$$

where a_1, a_2, a_3, and a_4 are defined by Eq. (10).

Apparently, if $p < h$ and $K < 0$, an arbitrary negative t makes the inequality Eq. (18) hold unless the $F/\#$ is sufficiently small such that the sign of the grouping of quantities in the parentheses is determined by the term of $y^4 t$, which is beyond the scope of this article. When $p < h$, $t < 0$ and paraxial optics are granted, $\Delta l_y(0)$ is exactly the minimum separated distance. The minimum absolute value of t is obtained as

$$-t \geq \frac{pRL_0}{2|p-h|d}. \tag{19}$$

4. SIMULATION AND CGH DESIGN EXAMPLES

A. Valuing the Accuracy of the Approximate Expressions

The approximate expressions of the CGH phase function, the shift Δy, and the separated distance Δl_y are derived based on the paraxial system assumption, i.e., $F/\#$ is large and K is small. Here, CGHs for four 2 m diameter $F/2$ conic surfaces with $K = -0.25$, -0.5, -0.75, and -1 are simulated with Zemax to evaluate the accuracy of the approximate expressions.

The phase function completely describes the diversity of the diffractive wavefront propagation and hence demands high calculation precision. The difference between the phase functions

calculated with Eq. (3) and the ray trace in Zemax is tiny, shown in Fig. 4. The error function is approximately axisymmetric, implying that the error is caused by the approximation made in Eq. (2) and the high-order spherical aberration. The error increases along with the increasing of the absolute value of y as expected. The maximum error, 0.02 mm at the boundary of the CGH when $K = -1$, is only 2.8% of the real value.

The approximate expression of shifts Δy proposed in this paper and the one obtained by Lindlein are compared with the ray-tracing simulation in Zemax, shown in Fig. 5(a). The former matches the practicalities better than the latter, evincing that the influence of the CGH position needs consideration. The effect of the conic constant K on the accuracy of the approximate expression of Eq. (6) is presented in Fig. 5. The error is positively correlated to the absolute value of K. The error mushrooms along the $-y$ direction, since the paraxial optics are considered and the tilt carrier frequency is along $+y$ direction, resulting in obvious error in the approximation $\sin\theta \approx \theta$ adopted to analyze the propagation directions of the diffractive wavefronts of the CGH when $y < 0$. The difference between the curves of the diffraction orders (0, 2) and (2, 0) is also mainly caused by the approximation $\sin\theta \approx \theta$.

In order to determine the amount of the needed tilt carrier frequency, the precision of the approximate expression of Δl_y is examined, shown in Fig. 6. It demonstrates that the precision of the approximate expression of Δl_y is satisfactory, especially when $-0.5 \le K \le 0$ or y is small, which is consistent with the paraxial hypothesis. Although the accuracy decreases when $y < 0$, similar to the expression of shifts Δy, only the accuracy when $y > 0$ is worth concentrating on, since it determines whether the parasitic diffraction orders are separated. The manifested difference between the curves of the separated distances Δl_y of the orders (0, 2) and (2, 0) is caused by the accumulation and magnification of the diversity of shifts Δy through twice diffraction, the nonlinear property of the CGH phase function shown in Fig. 4 and the fact that the shift $2\Delta y$ is comparable with y shown in Fig. 5. The samplings for the diffraction order (0, 2) do not spread all over the aperture, because the rays close to the CGH edge are blocked by the apertures of the CGH and the test mirror.

B. CGH Design Examples for Conic Surfaces

The paraxial model is applicable to both the Ronchi phase CGH and the chrome-on-glass amplitude CGH. Although the orders (−1, 3) and (3, −1) are the most disturbing diffraction-order combinations, because of the high diffraction efficiency [12], we concentrate on the disturbing orders (0, 2) and (2, 0) for two reasons. First, the separated distance Δl of the orders (0, 2) and (2, 0) is directly proportional to that of the orders (−1, 3) and (3, −1) according to Eq. (9). Second, because of fabrication errors in the grating depth and the duty cycle, the orders (0, 2) and (2, 0) will be different from zero, especially when an amplitude CGH is adopted, in which case it will significantly reduce the quality of the interferogram.

For a practical CGH, the spherical aberration brought in by the CGH glass substrate shifts the paraxial focus of the conic mirror. Assuming that the $F/2$ ellipsoid with $K = -0.25$ is under test, and the CGH is placed 7500 mm away, i.e., $h = 500$ mm, and fabricated on a 16.0 mm thick BK7 glass, the paraxial focus shifts 5.44 mm. Setting the filter plane 455.44 $(= 450 + 5.44)$ mm away from the CGH plane, while still treating $p = 450$ mm, and assuming the required minimum separated distance $L_0 = 0.5$ mm, the needed t is 9.5 mm according to Eq. (14). Actually, $t = 9.5$ mm is chosen. The CGH is designed with Zemax, shown in Fig. 7(a), and the parasitic waves are separated, shown in Fig. 7(b).

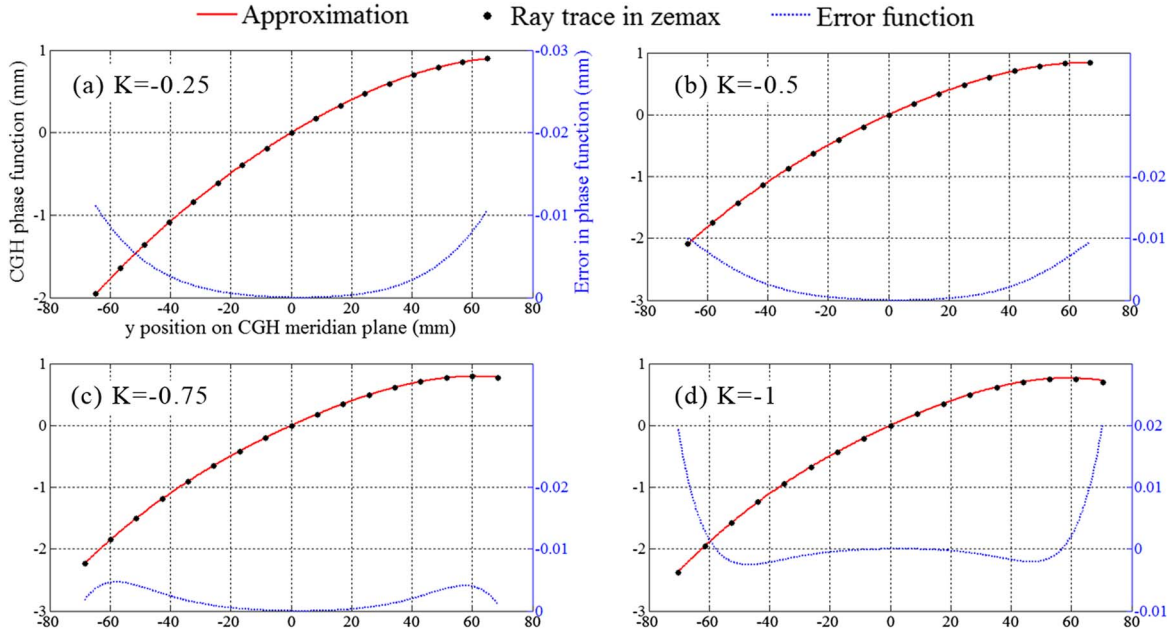

Fig. 4. Error in CGH phase function on the meridional plane versus $F/\#$. The error, defined as the approximate phase calculated with Eq. (3) minus the actual one gained by ray trace, shown as the blue dotted line, is drawn with respect to the ordinate on the right. The test optics are four 2 m $F/2$ conic surfaces with $K = -0.25$, −0.5, −0.75, and −1. CGHs are placed at the same position and loaded with the same tilt carrier frequency: $h = 500$ mm, $p = 450$ mm, and $t = 10$ mm.

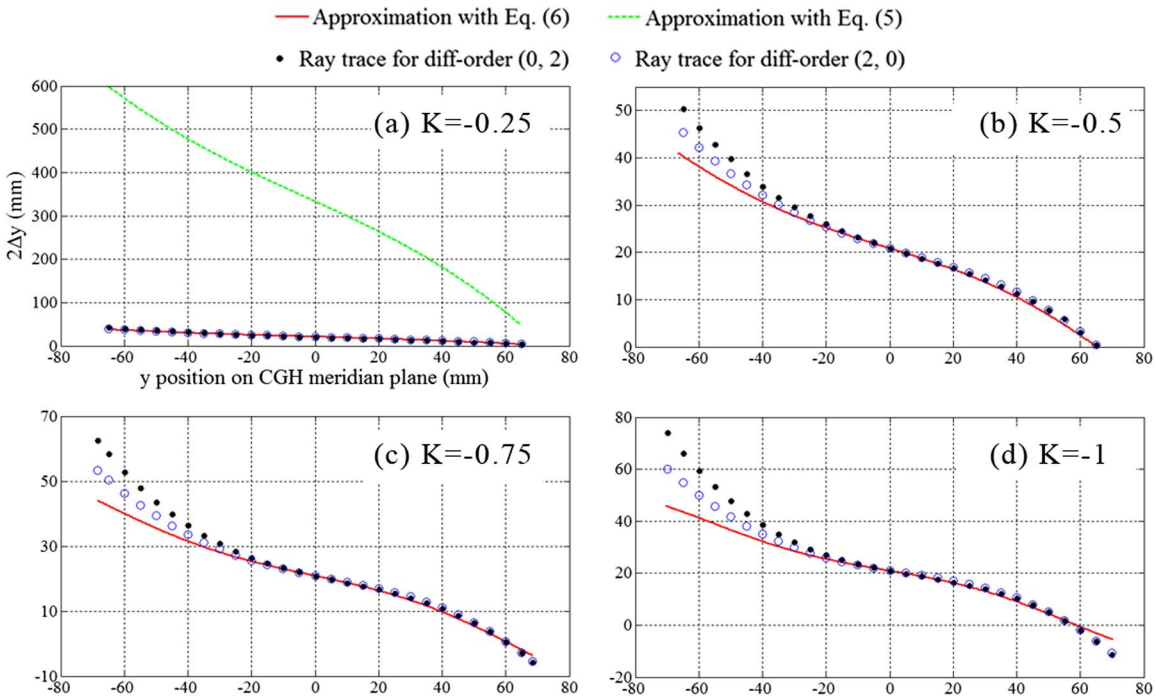

Fig. 5. Charts of the shifts $2\Delta y$ gained with Eqs. (5) and (6) and ray-tracing simulation. For brevity, the value $2\Delta y$ for the diff-order (0, 2) is shown after multiplying with −1. The curve calculated with Eq. (5) is only displayed in (a). But it sufficiently indicates that Eq. (5) is far away from the actual value. The approximate error is positively correlated to the absolute value of K, and grows rapidly along the $-y$ direction.

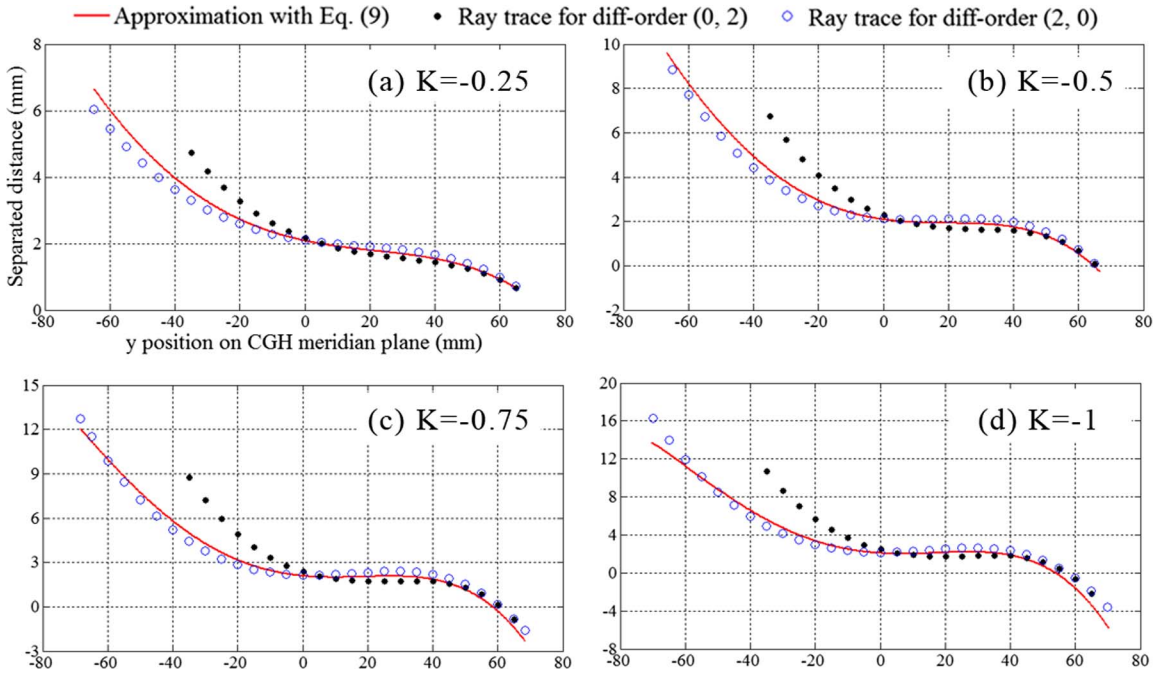

Fig. 6. Separated distances Δl_y of the rays with the diffraction order (0, 2) and (2, 0) on the meridian plane calculated with Eq. (9) and the ray trace show good agreement. The precision of Eq. (9) is acceptable when $-0.5 \le K \le 0$ or y is small. The samplings for the order (0, 2) do not spread all over the aperture, because the double-pass rays close to the edge are blocked. The semi-apertures of CGHs: (a) 64.8 mm, (b) 66.7 mm, (c) 68.5 mm, and (d) 70.3 mm.

The CGHs for the $F/2$ conic surfaces with $K = -0.5$, −0.75, and −1 are designed with the same method. The key parameters are exhibited in Table 1. In order to exclude the effect of the CGH glass plate, all the CGHs are designed on the 16 mm thick BK7 glass. These four CGHs are able to fabricate with high precision, since the sizes are less than 150 mm

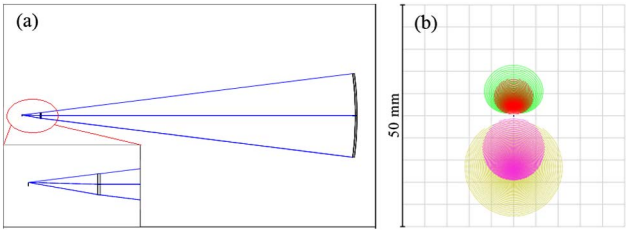

Fig. 7. (a) Design of a CGH used to test the 2 m diameter $F/2$ ellipse with $K = -0.25$. The CGH is fabricated on the right plane of the 16.0 mm thick BK7 glass substrate. $h = 500$ mm, $p = 450$ mm, and $t = 9.5$ mm. (b) Parasitic diffraction orders are separated on the filter plane, and typical orders are shown here. The separated distance: 0.5 mm for the order (0, 2) (red), 0.6 mm for the order (2, 0) (green), 1.2 mm for the order (0, 1) (purple), and 1.2 mm for the order (1, 0) (brown).

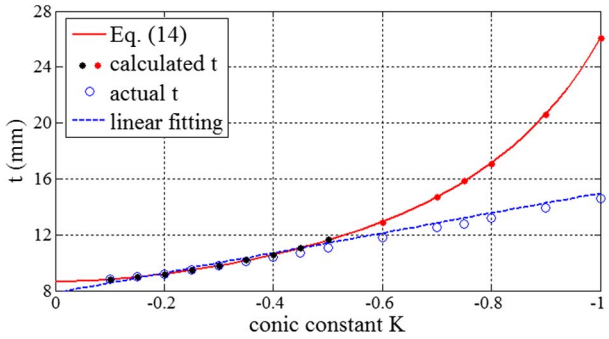

Fig. 8. Curves of the calculated t and the actual t versus K. The blue dotted line, obtained by linear fitting with the data of the calculated t when $-0.5 \le K < 0$ (the black solid sampling points), matches well to the actual t when $-1 \le K < 0.5$. The error between the fitted t and the actual t is among 0.3–0.4 mm when $-1 \le K < -0.5$.

and the minimum line spacing is larger than 10 μm [4,16]. The paraxial solution of Eq. (14) matches the practicalities well when $F/\# = 2$ and $-0.5 \le K \le 0$, with an error less than 5.1%, while the approximate error starts booming when $K \le -0.75$. It manifests that the approach can be applied for weak conic surfaces ($-0.5 \le K \le 0$) and the error decreases with the decreasing of the absolute value of K.

Notice that the actual t is nearly linear with the conic constant K, shown in Table 1, for the $F/2$ concave conic surfaces with $-1 \le K < -0.5$, the demanded t may be estimated through linear fitting with the data of the calculated t when $-0.5 \le K \le 0$. This method is illustrated in Fig. 8. The fitted curve, shown as the blue dotted line, matches the actual t well. The maximum error is about 0.4 mm. Certainly, the reason for the quasi-linearity between the actual t and conic constant K needs further investigation.

For the purpose of examining the error of Eq. (14) versus $F/\#$ of the test mirror and the thickness of the CGH, six CGHs are designed for the conic surfaces with $K = -0.5$ and $F/\# = 1.75$, 2, 2.25, and 2.5, displayed in Table 2. The maximum error is 12.1% when $F/\# = 1.75$, while the minimum error is 0.0% when $F/\# = 2.5$. Results suggest that the paraxial solution of Eq. (14) possesses high precision when $K = -0.5$ and $F/\# \ge 2$, with an error less than 5.1%. The error decreases as $F/\#$ increases, which is caused by paraxial optics treatment. It addresses that the approach can be applied for the conic surfaces with large $F/\#$($F/\# \ge 2$).

The two CGHs for the $F/1.75$ ellipsoid with thicknesses of 16.0 and 19.0 mm have the same approximate errors of 12.1%. Similarly, the errors of the CGHs for the $F/2.5$ ellipsoid with thickness distributions of 16.00 and 12.00 mm are both equal to 0.0%. The results imply that it is reasonable to ignore the influence of the CGH glass plate when determining the amount of the needed tilt carrier frequency.

The separated distance of the most disturbing diffraction-order combinations (−1, 3) and (3, −1) are examined and listed in Tables 1 and 2. The separated distance of order (−1, 3) is nearly four times that of the order (0, 2). This result is consistent with Eq. (9), indicating the feasibility of focusing on the orders (0, 2) and (2, 0). Parts of the rays with the orders (3, −1) and (2, 0) are blocked by the aperture of the test mirror, destroying the proportional relationship between them.

Table 1. Parameters of the Designed CGHs for the $F/2$ Conic Surfaces with $R = 8000$ mm ($h = 500$ mm, $p = 450$ mm)

Conic Constant		$K =$ −0.25	$K =$ −0.5	$K =$ −0.75	$K =$ −1
Approximate t (mm)		9.5	11.7	15.9	26.1
Actual t (mm)		9.5	11.1	12.8	14.6
Error (%)[a]		0.0	5.1	19.5	44.1
Separated Distance[b] (mm)	(0, 2)	0.5	0.5	0.5	0.5
	(2, 0)	0.6	0.7	0.8	1.0
	(0, 1)	1.2	0.9	0.7	0.5
	(1, 0)	1.2	0.9	0.7	0.5
	(−1,3)	1.9	2.0	2.0	2.0
	(3,−1)	3.2	4.8	7.3	11.4
CGH Thickness (BK7) (mm)		16.0	16.0	16.0	16.0
CGH Size[c] (mm)		129.7	133.4	137.0	140.6
Minimum Line Spacing (μm)		16.6	13.9	11.9	10.3

[a]Error(%) = |(Actual t − Approximate t)/Approximate t| × 100%.
[b]Includes the effect of apertures.
[c]Main CGH section.

C. CGH Design Example for a Concave Weak Aspheric Surface with a Large $F/\#$

The paraxial solution for the amount of the needed tilt carrier frequency is applicable to a concave weak aspheric surface with a large $F/\#$. Given a 2 m diameter $F/2$ aspheric surface with the fourth-order coefficient $A = -1.220 \times 10^{-13}$ mm^{-3}, $B = -1.691 \times 10^{-20}$ mm^{-5} is under test, setting $h = 500$ mm, $p = 450$ mm, and $L_0 = 0.5$ mm, the needed t is 11.9 mm according to Eqs. (14), (16), and (17). Actually, $t = 11.7$ mm (approximate error ~1.7%) is chosen to design the CGH with Zemax. The CGH pattern is fabricated on the right plane of the 16.0 mm thick BK7 glass substrate. The size of the CGH is 134.7 mm. The minimum line spacing is 13.1 μm. All the disturbing waves are separated: 0.5 mm for the order (0, 2), 0.6 mm for the order (2, 0), 0.8 mm for the order (0, 1),

Table 2. Parameters of the Designed CGHs for the Conic Surfaces with $K = -0.5$, $R = 8000$ mm ($h = 500$ mm, $p = 450$ mm)

$F/\#$		$F/1.75$		$F/2$	$F/2.25$	$F/2.5$	
Approximate t (mm)		15.7		11.7	9.5	8.2	
Actual t (mm)		13.8	13.8	11.1	9.4	8.2	8.2
Error (%)[a]		12.1	12.1	5.1	1.1	0.0	0.0
Separated Distance[b] (mm)	(0, 2)	0.5	0.5	0.5	0.5	0.5	0.5
	(2, 0)	0.8	0.8	0.7	0.7	0.7	0.7
	(0, 1)	0.7	0.7	0.9	1.1	1.2	1.2
	(1, 0)	0.7	0.7	0.9	1.1	1.2	1.2
	(−1,3)	2.0	2.0	2.0	2.1	2.0	2.0
	(3,−1)	5.4	5.4	4.8	4.2	3.7	4.1
CGH Thickness (mm)		16.0	19.0	16.0	16.0	16.0	12.0
CGH Size[c] (mm)		155.3		133.4	117.0	104.3	
Minimum Line Spacing (μm)		11.1	11.1	13.9	16.5	19.2	19.2

[a]Error(%) = |(Actual t − Approximate t)/Approximate t| × 100%.
[b]Includes the effect of apertures.
[c]Main CGH section.

and 0.8 mm for the order (1, 0). The design sketch for this CGH is not shown here, since it is similar to Fig. 7.

The approximate error of the amount of the needed tilt carrier frequency is only 1.7%, since the equivalent conic constant $K = a = -0.5$ and $F/\# = 2$ such that the paraxial optics are satisfied. The results are consistent with the data of the CGH for the $F/2$ conic surface with $K = -0.5$ shown in Table 1. The difference between the errors of 1.7% and 5.1% is caused by the effect of the sixth-order coefficient B and the intrinsic diversity of the conic constant K and the fourth-order coefficient A.

D. CGH Design Example for a Concave Off-Axis Aspheric Surface with a Weak Aspherical Deformation and a Large $F/\#$

Given a 1 m diameter concave off-axis aspheric surface with 0.5 m later displacement, $R = 8000$ mm, $A = -1.220\times 10^{-13}$ mm^{-3}, and $B = -1.691 \times 10^{-20}$ mm^{-5} is under test, still setting $h = 500$ mm, $p = 450$ mm, and $L_0 = 0.5$ mm, the needed t is −2.4 mm according to Eq. (19). The CGH is designed by choosing $t = -2.4$ mm, shown in Fig. 9(a). The CGH is fabricated on the 16 mm thick BK7 glass plate and placed perpendicular to the optical axis. The size of the CGH is 67.4 mm. The minimum line spacing is 22.1 μm. All the parasitic waves are separated, shown in Fig. 9(b): 0.5 mm for the order (0, 2) (red), 0.6 mm for the order (2, 0) (green), 2.4 mm for the order (0, 1) (purple), and 2.4 mm for the order (1, 0) (brown).

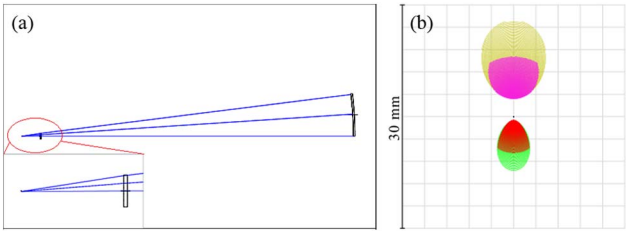

Fig. 9. (a) Design of a CGH used for the 1 m diameter off-axis aspheric surface with 0.5 m later displacement, $R = 8000$ mm, $A = -1.220 \times 10^{-13}$ mm^{-3}, and $B = -1.691 \times 10^{-20}$ mm^{-5}. The CGH is fabricated on the right plane of the 16.0 mm thick BK7 glass substrate. $h = 500$ mm, $p = 450$ mm, and $t = -2.4$ mm. (b) Parasitic diffraction orders are separated: 0.5 mm for the order (0, 2) (red), 0.6 mm for the order (2, 0) (green), 2.4 mm for the order (0, 1) (purple), and 2.4 mm for the order (1, 0) (brown).

The spots of the diffractive waves on the filter plane are spawn-liked [Fig. 9(b)], different from the circle ones of the on-axis aspherics [Fig. 7(b)]. This phenomenon is attributed to the off-axis aperture of the test mirror.

The approximate error for this off-axis aspheric surface is 0.0%. The reason is that only the rays coming from the CGH with position $y = 0$ contribute to determine the amount of the needed tilt carrier frequency, hence paraxial optics is naturally satisfied.

5. CONCLUSION

CGHs with tilt carriers placed outside the interferometer focuses are investigated in this paper. We have inherited and ameliorated Leidlein's work by containing the influence of the CGH position, and constructed a parametric geometric model to derive the phase function and the paraxial analytical solution for the amount of tilt carrier frequency needed to eliminate the unwanted waves. The paraxial analytical solution is applicable to concave weak aspheric surfaces ($-0.5 \le K \le 0$, where K includes the equivalent conic constant $K = a = 8AR^3$) with large f-numbers ($F/\# \ge 2$).

Simulations for several typical kinds of aspherics testing were conducted to compare the approximate expressions with the exact ray trace. Simulation results indicate that the approximate expressions are of high precision when K is small and $F/\#$ is large. For practical purposes, a study of the relationships among the approximate error of the amount of the needed tilt carrier frequency, the conic constant K, the $F/\#$ and the thickness of the CGH has been done. The approximate error is less than 5.1% when $-0.5 \le K \le 0$ and $F/\# \ge 2$, and vanishes when $K = -0.25$, $F/\# = 2$ or $K = -0.5$, $F/\# = 2.5$. The

effect of the CGH glass plate on the amount of the needed tilt carrier frequency is insignificant.

The results of this research show that the paraxial solution for the parameter t offers a reasonable recipe for separating the parasitic waves in the case that concave weak aspheric surfaces ($-0.5 \le K \le 0$, where K includes the equivalent conic constant $K = a = 8AR^3$) with large $F/\#(F/\# \ge 2)$ are under test, with an approximate error less than 5.1%. The linear fitting method can be applied when K and $F/\#$ are beyond the field of high accuracy. Besides, the necessary condition for separating the spurious diffraction orders provides a design guidance for selecting the proper position parameters h and p.

APPENDIX A

Equation (6) is derived as follows:

(a) The testing system is treated as paraxial optics, thus the shifts $\Delta\xi$ and $\Delta\eta$ on the aspheric surface are approximated as

$$\Delta\xi \approx \mathrm{AP}_x \cdot (m-1)\theta_x \approx (m-1)d\frac{\partial\Phi}{\partial x},$$
$$\Delta\eta \approx \mathrm{AP}_y \cdot (m-1)\theta_y \approx (m-1)d\frac{\partial\Phi}{\partial y}. \quad \textbf{(A1)}$$

(b) The shift of the local surface normal vectors from the point A to B, i.e., the included angle α, is obtained by the first-order approximation

$$\alpha_x \approx -\Delta\xi\frac{\partial N_x}{\partial\xi} - \Delta\eta\frac{\partial N_x}{\partial\eta},$$
$$\alpha_y \approx -\Delta\eta\frac{\partial N_y}{\partial\eta} - \Delta\xi\frac{\partial N_y}{\partial\xi}. \quad \textbf{(A2)}$$

(c) The length of $\mathrm{P}_m\mathrm{P}$ is approximately twice the length of MP based on the angle bisector theorem, hence the shifts Δx and Δy are given by

$$\Delta x \approx \mathrm{MP}_x \approx d(m-1)\theta_x - d\alpha_x,$$
$$\Delta y \approx \mathrm{MP}_y \approx d(m-1)\theta_y - d\alpha_y. \quad \textbf{(A3)}$$

(d) Paraxial optics are considered, hence $\xi, \eta \ll R$. The partial differentials of the surface normal vector $\mathbf{N}(\xi,\eta) = (N_x, N_y, 1)$ have the approximate expressions

$$\frac{\partial N_x}{\partial\xi} \approx -\frac{1}{R} - \frac{(K+1)(3\xi^2+\eta^2)}{2R^3} \approx -\frac{1}{R}, \qquad \frac{\partial N_x}{\partial\eta} \approx 0,$$
$$\frac{\partial N_y}{\partial\eta} \approx -\frac{1}{R} - \frac{(K+1)(3\eta^2+\xi^2)}{2R^3} \approx -\frac{1}{R}, \qquad \frac{\partial N_y}{\partial\xi} \approx 0. \quad \textbf{(A4)}$$

(e) Finally, the expressions of Δx and Δy are achieved by applying Eqs. (A1), (A2), and (A4) into Eq. (A3), shown as Eq. (6).

National High Technology Research and Development Program of China (863 Program) (863-2-5-1-13B).

Our deepest gratitude goes to the anonymous reviewers for their careful work and insightful comments that have helped improve this paper substantially.

REFERENCES

1. D. Malacara, *Optical Shop Testing*, 3rd ed., Vol. **59** of Wiley Series in Pure and Applied Optics (Wiley, 2007).
2. A. J. MacGovern and J. C. Wyant, "Computer generated holograms for testing optical elements," Appl. Opt. **10**, 619–624 (1971).
3. H. P. Stahl, "Aspheric surface testing techniques," Proc. SPIE **1332**, 66–76 (1990).
4. J. C. Wyant, "Computerized interferometric surface measurements," Appl. Opt. **52**, 1–8 (2013).
5. Z. Gao, M. Kong, R. Zhu, and L. Chen, "Problems on design of computer-generated holograms for testing aspheric surfaces: principle and calculation," Chin. Opt. Lett. **5**, 241–244 (2007).
6. J. H. Burge, "Advanced techniques for measuring primary mirrors for astronomical telescopes," Ph.D. thesis (University of Arizona, 1993).
7. J. Schwider, "Interferometric tests for aspherics," in *Fabrication and Testing of Aspheres*, Vol. **24** of OSA Trends in Optics and Photonics (Optical Society of America, 1999), paper T3.
8. G. S. Khan, K. Mantel, I. Harder, N. Lindlein, and J. Schwider, "Design considerations for the absolute testing approach of aspherics using combined diffractive optical elements," Appl. Opt. **46**, 7040–7048 (2007).
9. P. Zhou, J. H. Burge, and S. Peterhansel, "Optimal design of computer-generated holograms to minimize sensitivity to fabrication errors," Opt. Express **15**, 15410–15417 (2007).
10. S. Peterhänsel, C. Pruss, and W. Osten, "Phase errors in high line density CGH used for aspheric testing: beyond scalar approximation," Opt. Express **21**, 11638–11651 (2013).
11. Y. C. Chang, "Diffraction wavefront analysis of computer-generated holograms," Ph.D. thesis (University of Arizona, 1999).
12. N. Lindlein, "Analysis of the disturbing diffraction orders of computer-generated holograms used for testing optical aspherics," Appl. Opt. **40**, 2698–2708 (2001).
13. E. Garbusi and W. Osten, "Analytical study of disturbing diffraction orders in in-line computer generated holograms for aspheric testing," Opt. Commun. **283**, 2651–2656 (2010).
14. P. Zhou, W. Cai, C. Zhao, and J. H. Burge, "Parameteric definition for the CGH patterns and error analysis in interferometric measurements," Proc. SPIE **8415**, 841505 (2012).
15. P. Zhou, J. Burge, and C. Zhao, "Imaging issues for interferometric measurement of aspheric surfaces using CGH null correctors," Proc. SPIE **7790**, 77900L (2010).
16. W. Cai, P. Zhou, C. Zhao, and J. H. Burge, "Analysis of wavefront errors introduced by encoding computer-generated holograms," Appl. Opt. **52**, 8324–8331 (2013).